

PAPER • OPEN ACCESS

## Evaluation of the frost resistance of concrete in real operating conditions

To cite this article: S D Lapovska *et al* 2020 *IOP Conf. Ser.: Mater. Sci. Eng.* **907** 012039

View the [article online](#) for updates and enhancements.

# Evaluation of the frost resistance of concrete in real operating conditions

S D Lapovska<sup>1,3</sup>, G Iu Krasnianskyi<sup>2</sup>, V I Klapchenko<sup>2</sup> and I O Aznaurian<sup>2</sup>

<sup>1</sup>Chair of Building Materials, Construction Technology Department, Kyiv National University of Construction and Architecture, Kyiv, Ukraine

<sup>2</sup>Chair of Physics, Engineering Systems and Ecology Department, Kyiv National University of Construction and Architecture, Kyiv, Ukraine

<sup>3</sup>State Enterprise 'Ukrainian research, project planning and design institute of building materials and products', Kyiv, Ukraine

[aznaurian.io@knuba.edu.ua](mailto:aznaurian.io@knuba.edu.ua)

**Abstract.** The article proposes a method for evaluating the frost resistance of concrete at actual operating temperatures, using measurement results at temperatures that are regulated by current standards. Frost resistance was evaluated by determining the amount of water freezing at different temperatures, based on the measured adsorption isobars and the obtained relationship between the freezing temperature of water in concrete pores and relative humidity. A comparison of the calculated values of the frost resistance of concrete with those got based on direct measurements showed the adequacy of the calculation model. To get information about the frost resistance of concrete during unilateral freezing, a conductometric method was used to determine the kinetics of moisture diffusion and ice formation. It is shown that the use of this method allows one to establish the propagation speed of the ice formation and water diffusion front and the corresponding freezing depth of concrete samples depending on their capillary-porous structure and initial storage conditions. In general, the studies conducted allowed us to get a more reliable picture of the behaviour of concrete under alternating temperature load than is provided for by current regulatory documents.

## 1. Introduction

The frost resistance of building materials is determined by the current regulatory documents, which are based on the standard method of fixing the number of comprehensive freezing and thawing cycles for specially manufactured specimens that have not lost operational properties during testing. However, this approach does not always meet the requirements for the production of building materials and has a number of significant limitations.

The main problem is the mismatch of laboratory research conditions with the conditions in which this material is located in real structures. First, the maximum negative temperatures at which the structures are operated usually differ from the temperature of -18 °C at which tests are carried out under the current standard. In addition, in most cases, concrete structures undergo unilateral freezing, and a correlation relationship between this process and the comprehensive freezing process has not yet been found.

Modern ideas about the mechanisms of concrete destruction under the influence of frost (e.g., [1, 2]) are based on Powers' work. Obviously, one of the main causes of concrete damage during freezing is



the expansion of the water in the pores during its transition to ice. Powers suggested [3] that stresses leading to destruction can also cause hydraulic pressure when water moves from frozen areas. At the same time, there are other reasons that are not associated with an increase in the volume of water during crystallization, causing destructive deformation of concrete [4].

The super-cooled liquid in the gel pores has greater free energy than the ice in the capillaries. As a result, it is transferred to the capillaries with an increase in the volume of ice in them, which leads to additional internal stresses in the concrete. Moreover, due to the difference in salt concentration caused by freezing water in large pores, osmotic pressure arises, which also leads to concrete damage.

Since the root cause of the mechanisms of frost destruction of concrete is still the expansion of water during its transition to ice, it can be expected that the frost resistance of the material, expressed by the number of cycles, with a change in the maximum freezing temperature, should be inversely proportional to the volume of frozen water in the material at this maximum temperature. This is also consistent with the known semi-empirical correlations between frost resistance and ice content in concrete [5].

It is known that in concrete, which is subjected to unilateral freezing in real conditions of operation, because of the heterogeneity of moisture distribution, intensive mass transfer processes are taking place. These processes significantly affect the resistance of concrete to alternating temperature loads. At the same time, conductometric methods are highly sensitive to physicochemical processes occurring in concrete, in particular, such as changing the phase state of pore moisture, its chemical composition, concentration, and temperature [6].

Because of this, conductivity measurements can be used to obtain additional information on the frost resistance of concrete during unilateral freezing. The observed features of the conductivity behavior can be interpreted based on existing ideas about the kinetics of ice formation and moisture diffusion in capillary-porous materials [7, 8].

## 2. Experimental

Experimental verification of the proposed method for evaluating the frost resistance of concrete at different freezing temperatures was carried out on expanded clay concrete specimens. To prepare the concrete specimens, CEM I 42,5 N cement according to the Ukrainian standard DSTU B EN 197-1:2015, expanded clay according to DSTU B V. 2.7-17, quartz sand according to DSTU B V.2.7-32-95 were used. To determine frost resistance, concrete specimens were made according to DSTU B V. 2.7-214:2009 and DSTU B V. 2.7-18-95.

The dimensions of the specimens were 100×100×100 mm. Three sets of specimens of different density of six pieces each were made. In the set 1 –  $\rho_1 = 1450 \text{ kg}\cdot\text{m}^{-3}$ , in the set 2 –  $\rho_2 = 1650 \text{ kg}\cdot\text{m}^{-3}$ , in the set 3 –  $\rho_3 = 1960 \text{ kg}\cdot\text{m}^{-3}$ .

Examinations of frost resistance were conducted according to DSTU B V. 2.7-47-96. The frost resistance of concrete is equal to a certain number of freezing-thawing cycles of water-saturated specimens, at which concrete compressive strength is reduced by no more than 15 %, and specimen mass loss does not exceed 5 %.

Frost resistance determination method involves cyclic freezing of the specimens in the air with a temperature of  $-18 \pm 2 \text{ }^\circ\text{C}$  for at least 4 hours and then defrosting under the water at room temperature for at least 4 hours. For research, frost resistance was also measured at temperatures from  $-5$  to  $-40 \text{ }^\circ\text{C}$ , which differ from the standard.

The measurements of the equilibrium water-holding characteristics of the experimental expanded clay concrete specimens were carried out by the known method for the determination of adsorption isobars [9]. For this purpose, ground concrete specimens at a temperature  $t_1$  were blown with air saturated with water vapour at a lower temperature  $t_2$ . The relative humidity  $\varphi$  at which the specimens were located was calculated by the formula:

$$\varphi = \frac{p_s(t_2)}{p_s(t_1)}, \quad (1)$$

where  $p_s(t_1), p_s(t_2)$  – saturated water vapor pressure at temperatures  $t_1$  and  $t_2$ , respectively.

The equilibrium moisture contents of the specimens  $U_\varphi$  were calculated by their masses measured by the weight method:

$$U_\varphi = \frac{m_\varphi - m_0}{m_0}, \quad (2)$$

where  $m_\varphi$  – the mass of specimen in equilibrium with air having relative humidity  $\varphi$ ,  $m_0$  – dry mass.

The maximum moisture content  $U_m$  of the specimens were calculated as the relative amount of moisture absorbed by the porous material upon its contact with water in relation to the dry mass  $m_0$  of the material:

$$U_m = \frac{m_s - m_0}{m_0}, \quad (3)$$

where  $m_s$  – mass of water-saturated specimen.

The kinetics of ice formation and moisture migration during unilateral freezing were investigated on hardened cement mortar specimens after 28 days of maturation. The dimensions of the specimens were 40×40×80 mm. Stainless steel electrodes with a diameter of 2.5 mm were placed into the upper and lower faces of the samples during formation at a distance of 1 cm from each other.

Electrical conductivity measurements were performed at an alternating current frequency of 10 kHz according to the method described in [6]. Specimens subjected to unilateral freezing were placed in a heat-insulating cassette. Before measuring, some samples were saturated with water at room temperature for 48 hours, and some were kept in the air. The passage of moisture was fixed by the salt mark method, for which a warm end of the sample was moistened with a 4 % solution of sodium chloride in water.

### 3. Results and discussion

In the paper, frost resistance of concrete at various freezing temperatures was evaluated by the experimental-analytical method, which is based on the assumption that frost resistance, expressed in the number of cycles (F), should be inversely proportional to the volume of frozen water at this temperature:

$$F(t_2) = F(t_1) \cdot \frac{V(t_1)}{V(t_2)}, \quad (4)$$

where  $V(t_1)$  and  $V(t_2)$  – volumes of frozen water at maximum freezing temperatures  $t_1$  and  $t_2$ .

The amount of water frozen at different temperatures is uniquely determined by the thermodynamic characteristics of its bond in the material. The data needed to calculate  $V(t)$  are most easily calculated from the water vapour adsorption isobar. Isobar takes into account the decrease in the freezing temperature of water both because of the curvature of the meniscus of water in the pores, and because of dissolved electrolytes. Therefore, there is no need to introduce any corrections to the change in the freezing temperature of the pore solution (at its low concentration). In addition, the adsorption isobar can be measured at any temperature, for example, at room temperature, since the chemical bond potential of water, which determines the decrease in the freezing temperature, is practically independent of temperature. The measured water vapour adsorption isobars are shown in figure 1.

The volume of frozen water increases with increasing negative temperature, although monotonously, but sharply nonlinear, since the adsorption isobar itself is usually nonlinear. Therefore, the change in frost resistance at different temperature ranges can be significantly different.

Since the isobar, as a rule, is set graphically (measured in the experiment), it is not possible to write the formula for calculating frost resistance at different temperatures in a general form. The calculation has to be carried out sequentially by determining the amount of frozen water and the corresponding frost resistance.

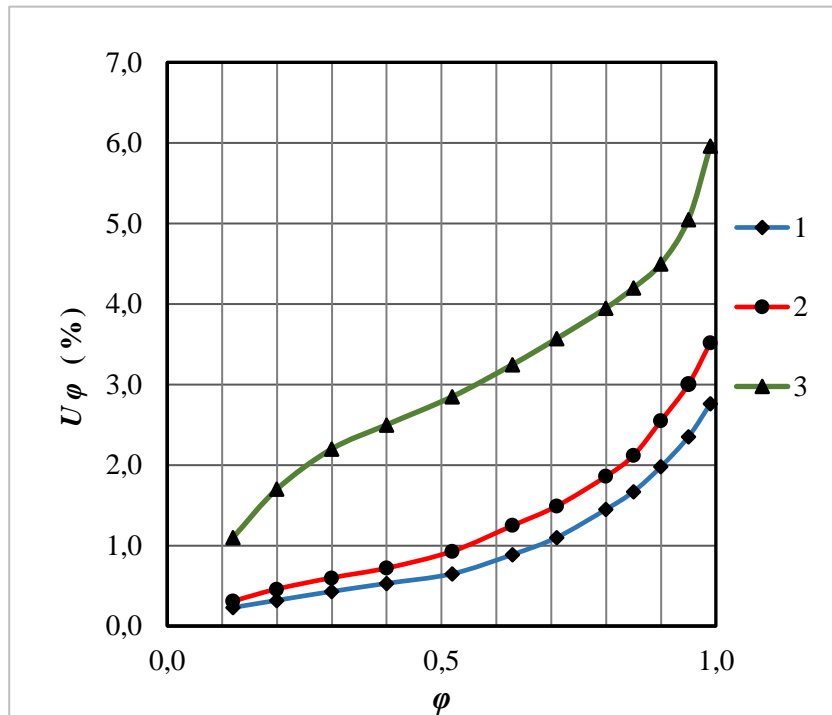


**Figure 1.** Adsorption isobars of expanded clay concrete specimens (the numbering of the curves corresponds to the table 1).

Evaluation of frost resistance was carried out according to the following scheme. Initially, the ratio of the volumes of water freezing in the specimen at given temperatures  $t$  was determined:

$$\frac{V(t_1)}{V(t_2)} = \frac{U_m - U_{\phi 1}}{U_m - U_{\phi 2}} \tag{5}$$

The expression for the relative humidity  $\phi$  corresponding to a given freezing temperature of water in the pores of the material can be derived from the Gibbs – Thomson equation. With a hemispherical interface between ice and a non-wetting liquid in a pore of radius  $r$ , the Gibbs – Thomson equation for the freezing temperature reduction can be written in the form [10,11]:

$$\Delta T = T_{\infty} - T = -T_{\infty} \cdot \frac{2\sigma_{il} \cdot \cos \theta}{\Delta H_m \cdot r \cdot \rho_i} \tag{6}$$

where  $T$  is the absolute melting temperature of the ice in a pore of radius  $r$ ;  $T_{\infty}$  is the bulk melting temperature of ice;  $\sigma_{il}$  is the specific surface energy at the ice-liquid interface;  $\Delta H_m$  is the specific melting enthalpy;  $\rho_i$  is the density of the ice;  $\theta$  is the contact angle (usually considered  $\theta = 180^\circ$ ).

Then, using the Ostwald – Freundlich equation:

$$\ln \phi = \frac{2\sigma \cdot V_{\mu}}{RT \cdot r} \tag{7}$$

where  $\sigma$  is the liquid surface tension,  $V_{\mu}$  is the molar volume,  $R$  is the gas constant, for the value of relative humidity  $\phi$  at which the absolute freezing temperature is  $T$ , we get:

$$\varphi = \exp \left[ \left( \frac{1}{T_\infty} - \frac{1}{T} \right) \cdot \frac{L \cdot \mu}{R} \right], \tag{8}$$

where  $\mu$  is the molar mass of water.

Dependence (8) was obtained under the assumption that  $\sigma = \sigma_{ii}$  and when  $\Delta H_m = L$  is taken into account, where  $L$  is the specific melting heat of ice. A similar expression for the dependence of the phase transition temperature in the capillary on the relative vapour pressure was obtained in [12] from the Clausius – Clapeyron relation.

It is necessary to keep in mind that in the derivation of (8) it was assumed that the freezing temperature of the liquid is calculated in a water-saturated capillary-porous material with a rigid skeleton. We also note that in calculating the values of relative humidity corresponding to certain freezing temperatures and volumes of frozen water, the dependence of melting heat of ice  $L$  on temperature was neglected. And although in the temperature range studied,  $L$  can vary up to 20 % [13], this, as estimates show, does not introduce a significant error in the calculations.

After calculating the volumes of water freezing in the specimens at given temperatures, the values of frost resistance at different freezing temperatures were calculated using formula (4), choosing the value of  $F$  at  $-18\text{ }^\circ\text{C}$  as the base point. The calculation was performed for each of the six specimens of each set. The experimental and calculated values of frost resistance of expanded clay concrete specimens at different temperatures are shown in the table and in figure 2.

**Table 1.** The experimental and calculated values of frost resistance of expanded clay concrete specimens at different freezing temperatures

$t$ ( $^\circ\text{C}$ )	$F$ , cycles - average values					
	set 1 ( $U_m=3,02\%$ )		set 2 ( $U_m=4,12\%$ )		set 3 ( $U_m=6,55\%$ )	
	exp.	calc.	exp.	calc.	exp.	calc.
-5		49	78	77		123
-10	36	32	59	55	98	90
-18	23	-	41	-	75	-
-35		17	34	32		60
-40		16	25	30		57

The frost resistance values found by direct measurements and calculation differ for each set no more than the experimental frost resistance values for specimens of one set. These data confirm the possibility of using the proposed method of evaluation of the frost resistance of concrete at different freezing temperatures and, accordingly, the fairness of the model calculation. Moreover, they show that, apparently, the same mechanism of frost destruction prevails in the studied temperature range from 0 to  $-40\text{ }^\circ\text{C}$ .

Based on the research data, it is possible to evaluate the frost resistance of concrete and other building materials at any temperature using the measurement results at a temperature of  $-18\text{ }^\circ\text{C}$ , which is regulated by current standards. Such a calculation can significantly save time and costs compared with those in a direct experiment.

For a more detailed study of the mechanisms of frost destruction of building materials, it is necessary to have at the same time information on the kinetics of ice formation and moisture migration in the process of their unilateral freezing. The following shows the possibility of determining the propagation velocity of the ice formation front and moisture diffusion in building materials using the conductometric method. The arrangement of electrode pairs in the tested specimens is shown in figure 3, and the results of measurements of the electrical conductivity  $\sigma$  are shown in figure 4 and figure 5.

As seen from figure 4, the electrical conductivity of the specimen, which was before the experiment under conditions of air storage, varies in different sections of the specimen according to different laws. The same dependences  $\sigma(\tau)$  are observed for a water-saturated specimen with the only difference being that the changes in conductivity that occur in the corresponding time intervals are much less pronounced.

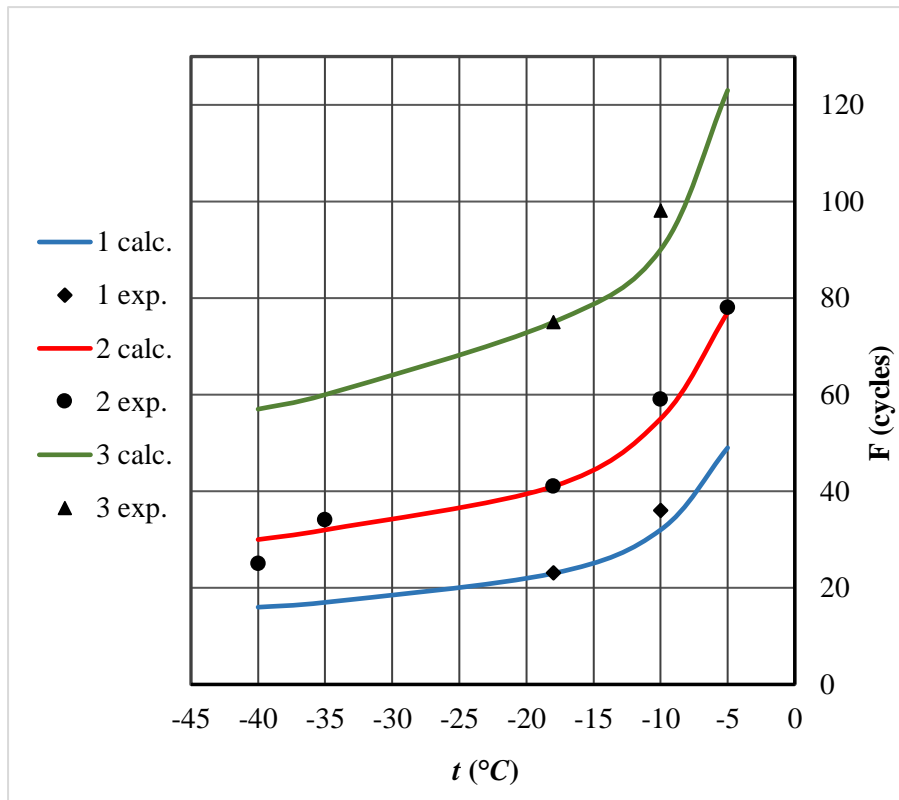


**Figure 2.** Dependence of frost resistance of expanded clay concrete specimens on freezing temperature (the numbering of the curves corresponds to the table).

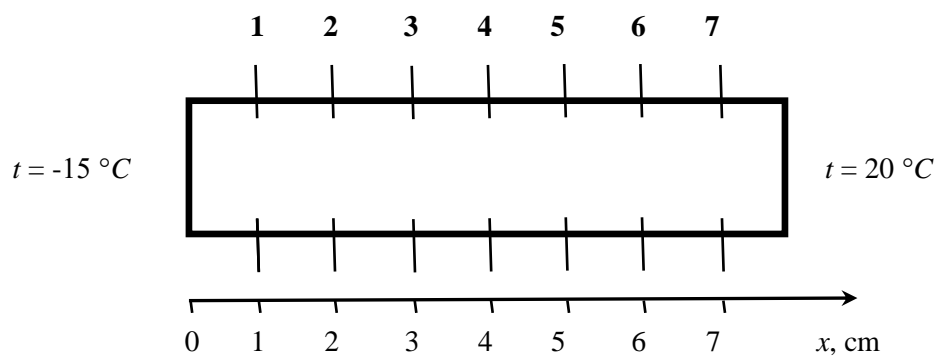


**Figure 3.** Experimental hardened cement mortar specimen (1...7 – electrode pair number).

At the initial time, the temperature is the same along the entire length of the specimen, and the moisture in its pores is in equilibrium. This corresponds to almost coinciding values of  $\sigma$  for all sections of the specimen. Then, the process of ice formation, starting from the frosty face of the specimen, is accompanied by the establishment of a temperature gradient and the appearance of thermal and concentration diffusion of moisture. In this case, the corresponding diffusion flows are directed to the side opposite to the direction of ice formation front propagation.

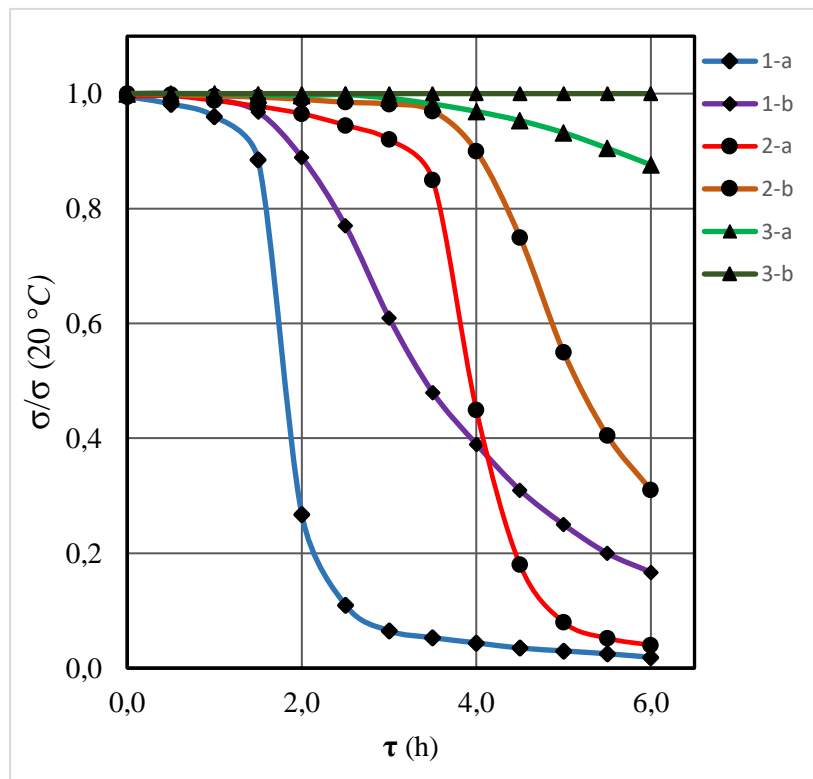


**Figure 4.** Dependence of electrical conductivity of mortar specimen on freezing time: a – water-saturated specimen; b – air-stored specimen (the numbering of the curves corresponds to electrode pair numbers).

It is known [14] that when the temperature changes the electric conductivity of cement mortar and concrete changes according to the exponential law. Thus, the reduction of temperature in some section of the specimen over time should lead to the fall of the  $\sigma$ . The conductivity should also be reduced because of a decrease in moisture content in the corresponding zone caused by thermal moisture transfer. A lower temperature and a larger temperature gradient near the cold face of the specimen cause redistribution of moisture over the volume of the specimen so that a concentration gradient is created that coincides in direction with the temperature gradient. At the same time, the indicated decrease in moisture content can be compensated by the displacement of unfrozen water to the considered region during ice formation. The observed slight decrease in conductivity at the initial stage of cooling shows the predominant contribution of the first two of the described mechanisms.

A sharp decrease in the conductivity at the locations of the electrode pairs 1 and 2 shows the achievement of these sections of the specimen by the ice formation front since the specific electrical conductivity of ice is much lower than the specific electrical conductivity of pore moisture. A smaller change in conductivity in the indicated time interval for a water-saturated specimen can be explained based on the following considerations.

When water-saturated concrete is frozen, ice formed in the surface zone creates increased pressure in the displaced liquid phase, because of which the ice formation temperature decreases. Thereby, at the same temperature, the ice content of the water-saturated specimen should be lower and its contribution to the change in conductivity, decreases.

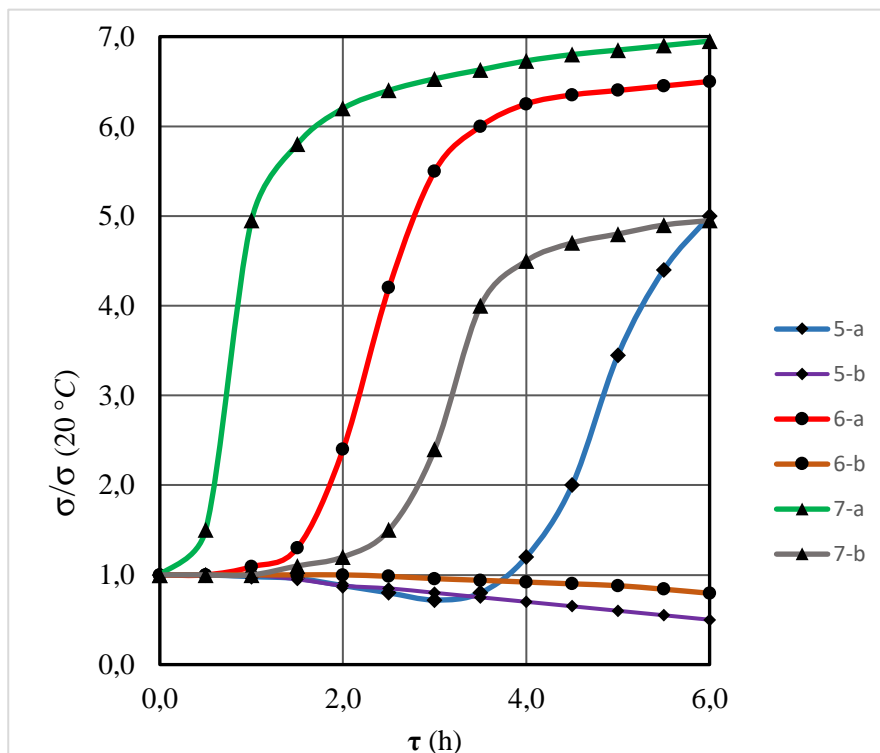


**Figure 5.** Dependence of electrical conductivity of mortar specimen on freezing time: a – water-saturated specimen; b – air-stored specimen (the numbering of the curves corresponds to electrode pair numbers).

An analysis of experimental data shows that during the measurements, the ice front does not reach the zone of the third electrode pair, although, based on the kinetics of ice formation, the duration of the experiment for this may be sufficient. This circumstance, apparently, is explained by the following. By the time the measurements are completed, the concentration of salt coming from the wetted face of the specimen increases in the indicated zone, which leads to a slowdown in the freezing process. This also allows us to conclude that the nature of changes in conductivity in the zones of the 5th, 6th, and 7th electrode pairs (figure 5) should reflect the kinetics of moisture transfer in the specimens during unilateral freezing.

Indeed, a sharp increase in electrical conductivity in sections 6 and 7 is apparently associated with a growth in moisture content and an increase in the concentration of the salt solution. By the time the salt mark arrives in section 6, the temperature in it has time to become lower than in section 7, which leads to lower values of conductivity hereafter. In this time interval, the influence of salt flow in section 5 has not yet been observed. And since the temperature here decreases, a slight decrease in the conductivity occurs (curve 5-a).

It follows from figure 5 that changes in the conductivity in the corresponding sections of a water-saturated sample occur much more slowly and their value is much smaller. To explain these features, it is necessary to take into account that the change in moisture content here can only be caused by thermal and moisture conductivity, whose role at high temperatures and low-temperature gradients in the considered region of the specimen should be small. In this case, the movement of the salt mark occurs because of the diffusion of salt from the wetted face of the specimen. Thus, an increase in the electrical conductivity in section 7 is apparently associated mainly with a growth in the salt concentration, and a decrease in the electrical conductivity in sections 5 and 6 should occur because of a decrease in temperature.

Comparing the measurement results, we can conclude that the average speed of the ice formation front during unilateral freezing of a mortar specimen of the investigated composition does not depend on the initial moisture content and 6 hours after the start of freezing is 0.4 cm/h. At the same time, the average speed of the salt mark in such a specimen for the same time decreases when the specimen is saturated with water, changing from 0.5 cm/h for an air storage specimen to 0.2 cm/h for a specimen subjected to water saturation in within 48 hours.

#### 4. Conclusions

The proposed experimental-analytical method for evaluating the frost resistance of concrete at different freezing temperatures allows in a small amount of time to get more complete information about the behavior of the material in frosty weather under real operating conditions than is provided for by existing methods. An analysis of the dependence of frost resistance on temperature also makes it possible to identify the temperature regions where it changes most strongly, and to shift, if necessary, these regions to lower or higher temperatures due to the change of the composition and technology of concrete production.

Moreover, the developed combined method for the independent measurement of the kinetics of moisture diffusion and the ice formation allows one to determine the rates of these processes depending on the composition (capillary-porous structure) of the specimens and the initial storage conditions. Such information can give a more reliable picture of the behavior of concrete under alternating temperature load in conditions of different initial moisture content (including in hydraulic structures) than current regulatory documents allow.

#### 5. References

- [1] Ramachandran V S, Feldman R F and Beaudoin J J 1981 *Concrete Science: Treatise on Current Research* (London: Heyden)
- [2] Neville A M and Brooks J J 2010 *Concrete Technology* (Harlow: Prentice Hall)
- [3] Powers T C 1945 Basic considerations pertaining to freezing and thawing tests *Proc. Am. Concrete Inst.* **41** 245-272
- [4] Powers T C and Helmuth R A 1953 Theory of volume changes in hardened Portland cement paste during freezing *Proc. Highw. Res. Board* **32** 285-297
- [5] Dvorkin L, Dvorkin O and Ribakov Yu 2013 *Multi-Parametric Concrete Compositions Design* (New York: Nova Science Publishers Inc.)
- [6] Krasnianskiy G, Aznaurian I and Kucherova G 2013 Methods of electrophysical research of concrete in the early stages of hardening *Mistobuduvannya ta terytorialne planuvannya* **50** 310- 315
- [7] Feldman G M 1988 *Moisture Movement in Thawed and Freezing Soils* (Novosibirsk: Nauka)
- [8] Gorchakov G I, Kapkin M M and Skramtaev B G 1965 *Improving the Frost Resistance of Concrete in the Industrial and Hydraulic Structures* (Moscow: Stroyizdat)
- [9] Gregg S J and Sing K S W 1982 *Adsorption, Surface Area and Porosity* (London: Academic Press)
- [10] Jackson C L and McKenna G B 1990 The melting behavior of organic materials confined in porous solids *J. Chem. Phys.* **93** 9002-9011
- [11] Webber J B W 2010 Studies of nano-structured liquids in confined geometries and at surfaces *Progress in Nuclear Magnetic Resonance Spectroscopy* **56** 78-93
- [12] Krasilnikov K G, Nikitina L V and Skoblinskaya N N 1980 *Physico-chemistry of Own Deformations of Cement Stone* (Moscow: Stroyizdat)
- [13] Feistel R and Wagner W 2006 A new equation of state for H<sub>2</sub>O ice Ih *J. of Phys. Chem. Reference Data* **35** 1021-47
- [14] Bernatsky A F, Celebrovsky Yu V and Chunchin V A 1980 *Electrical Properties of Concrete* ed Yu N Vershinina (Moscow: Energy)